



Inner radiation belt source of helium and heavy hydrogen isotopes

A.A. Leonov^{a,*}, A.M. Galper^a, S.V. Koldashov^a, V.V. Mikhailov^a, M. Casolino^b,
P. Picozza^b, R. Sparvoli^b

^a *Moscow Engineering Physics Institute (State university), Kashirskoe Shosse 31, Moscow, 115409, Russia*

^b *University of Rome "Tor Vergata" and INFN Section of Roma2, Via della Ricerca Scientifica, 1, I-00133 Rome, Italy*

Received 16 September 2004; received in revised form 13 July 2006; accepted 9 September 2006

Abstract

Nuclear interactions between inner zone protons and atoms in the upper atmosphere provide the main source of energetic H and He isotope nuclei in the radiation belt. This paper reports on the specified calculations of these isotope intensities using various inner zone proton intensity models (AP-8 and SAMPEX/PET PSB97), the atmosphere drift-averaged composition and density model MSIS-90, and cross-sections of the interaction processes from the GNASH nuclear model code. To calculate drift-averaged densities and energy losses of secondaries, the particles were tracked in the geomagnetic field (modelled through IGRF-95) by integrating numerically the equation of the motion. The calculations take into account the kinematics of nuclear interactions along the whole trajectory of trapped proton. The comparison with new data obtained from the experiments on board RESURS-04 and MITA satellites and with data from SAMPEX and CRRES satellites taken during different phases of solar activity shows that the upper atmosphere is a sufficient source for inner zone helium and heavy hydrogen isotopes. The calculation results are energy spectra and angular distributions of light nuclear isotopes in the inner radiation belt that may be used to develop helium inner radiation belt model and to evaluate their contribution to SEU (single event upset) rates.

© 2006 Published by Elsevier Ltd on behalf of COSPAR.

Keywords: Inner magnetosphere; Trapped energetic particles; Isotopes; Atmospheric composition and structure

1. Introduction

The flux of energetic light ions at low altitude is both an important input and output to self-consistent calculations of albedo particles resulting from the interaction of trapped and cosmic ray particles with the upper atmosphere. In addition, data on the flux of light ions are needed to evaluate radiation damages on space-borne instruments and space mission crew. The measurements and modelling of the flux of energetic alpha-particles would help to assess their direct or indirect contribution to SEU production in sensitive electronic devices at low Earth orbit (Dodd and Massengill, 2003).

As it is well known protons present the main inner radiation belt component. The nuclear interaction of the

trapped protons with the atoms of the upper atmosphere is the source of H and He isotopes. If the pitch-angle of a generated particle lies outside the loss cone on the given geomagnetic shell this particle becomes trapped. It was shown (Galper et al., 2003; Pugacheva et al., 1998; Seleznick and Mewaldt, 1996) that such processes provide the main source of high-energy geomagnetically trapped ²H, ³H, ³He and ⁴He nuclei at L-shell < 1.3.

This paper reports on the improved calculations of intensities of secondary light nuclei isotopes deduced from: the inner zone proton intensity obtained out of empirical models AP-8 and SAMPEX/PET PSB97; the atmosphere drift-averaged composition and densities from dynamic atmosphere model MSIS-90, and double-differential cross-sections for the various nuclear interaction processes extracted from GNASH nuclear model code. The calculation results are the energy spectra and angular distributions of deuterium and helium-4 nuclei in the inner radiation belt

* Corresponding author. Tel.: +7095 3239251; fax: +7095 3239281.
E-mail address: alexeyanatolievich@rambler.ru (A.A. Leonov).

that may be used to develop helium inner radiation belt model and to evaluate light nuclear contribution to SEU rates.

2. Method of calculations

For L-shell less than 1.3 the atmospheric production of energetic secondary nuclei is balanced only by ionization energy loss in the atmosphere, as the radial diffusion is not significant at this region (Pugacheva et al., 1998). The intensity j of generated particles satisfies a continuity equation (Jentsch and Wibberenz, 1980):

$$\frac{1}{v} \times \frac{\partial j}{\partial t} = S + \frac{\partial}{\partial E} (j \times \left| \frac{dE}{dx} \right|),$$

where v is the nonrelativistic particle speed at time t and kinetic energy E ; the production rate is S ($\text{cm}^3 \text{ s sr MeV}^{-1}$). In stationary case this equation has solution:

$$j = \frac{1}{\left| \frac{dE}{dx} \right|} \int_E^\infty S dE. \quad (1)$$

During the longitude drift trapped proton performs great number of oscillations between mirror points. Therefore, if the drift-averaged atmospheric density n_i of given type target atoms is known as function of trapped particle guide center location along the field line, then the expression for production rate of secondary nuclei can be writing in the following way (Galper et al., 2003; Selesnick and Mewaldt, 1996):

$$S(E, \alpha, L) = \int_{t_m}^{t'_m} dt \sum_i \int dE_p \int d\Omega_p [x(t)] \times n_i[x(t)] \times j_p \times \frac{d^2 \sigma_i}{d\Omega dE} / \int_{t_m}^{t'_m} dt. \quad (2)$$

The first integral covers the time interval $[t_m, t'_m]$ over which the guiding center of trapped proton performs one oscillation between mirror points x_m and x'_m . The summation extends over all interactions that lead to a given type of secondary particle and the following integrals cover the ranges of the proton energies E_p and the solid angle Ω_p that kinematically can produce secondaries with energy E , equatorial pitch-angle α in a solid angle $d\Omega_{\text{eq}}$, and at given L-shell. The proton intensity is j_p , and the cross-section for interaction i is σ_i . The values of cross-sections were defined from nuclear model code GNASH (Young et al., 1992), which includes the double-differential emission spectra in the laboratory frame. Replacing first integral in Eq. (2) by the sum over various regions of guide center trajectory between the mirror points x_m and x'_m one can get (Galper et al., 2003):

$$S(E, \alpha, L) = \sum_j \sum_i \int dE_p \int d\langle \Omega_p \rangle_j \times \langle n_i \rangle_j \times j_p(\alpha_p, E_p, L) \times (d^2 \sigma_i / d\Omega dE). \quad (3)$$

In Eq. (3), $\langle \Omega_p \rangle_j$ is the average solid angle of trapped protons at j th region of the guide center trajectory corre-

sponding to the given equator pitch-angle α_p ; $\langle n_i \rangle_j$ is a drift-averaged atomic concentration of i th atmospheric constituent on the same trajectory region. Each j th region is defined by range of a local proton pitch-angles α'_p corresponding to the fixed proton equatorial pitch-angle α_p . By this the calculations account for the nuclear interaction kinematics along the whole trajectory of guide centre of trapped proton between the mirror points. This allows correctly take into account the generation of secondary particles nearby the mirror points where the atmosphere density is largest. This approach differs from that one used by Selesnick and Mewaldt (1996), where n_i was constant for the chosen equator pitch-angle α_p . The drift-averaged density of atmosphere component i at the given trajectory region j is:

$$\langle n_i \rangle_j = \int_{t_j} n_i(\alpha'_p(t)) dt / \int_{t_j} dt, \quad (4)$$

where t_j – drift time at the given proton trajectory region j ; t_{Dr} – time of the total longitude proton drift.

To calculate the drift-averaged densities of different atmosphere components the protons were traced in the geomagnetic field as described by the IGRF-95 model (Barton, 1996) by numerical solution of motion equation. Atmospheric densities were defined from dynamic atmosphere model MSIS-90 (Hedin, 1991) with input parameters: AP = 4, F10.7 = 140. The values of these parameters were obtained using the averaging over the time period of NINA experiment. Similarly, to define the average energy losses of secondary nuclei their trajectories in the geomagnetic field were modelled.

Fig. 1 shows the dependence of the drift-averaged concentrations of the main atmospheric constituents from an equator pitch-angle of trapped protons with energy 350 MeV (a) and the dependence of drift-averaged concentrations of the atmospheric helium from the local and equator pitch-angle of trapped protons with energy 100 MeV (b) on L-shell 1.2 calculated using Eq. (4).

To define the production rate from Eq. (3) it is necessary to know the proton intensity j_p . At the present there are different estimations of this value. Fig. 2 shows the energetic directional spectrum of trapped protons for solar minimum at L-shell 1.2, derived from the different most known trapped protons models: AP-8 (Gaffey and Bilitza, 1994) and SAMPEX/PET PSB97 (Heynderickx et al., 1999). To get the intensity of trapped protons from the omnidirectional fluxes in AP-8 models the following transformation was used (Selesnick and Mewaldt, 1996):

$$j_p = \frac{1}{2\pi^2} \frac{\partial^2}{\partial E \partial x} \int_0^x \frac{J_p(E, x')}{(x - x')^{1/2}} dx', \quad (5)$$

where $x = B_0/B$ (B_0, B – magnetic field values at equator and current point on the given force line correspondingly); J_p is omnidirectional proton intensity. Fig. 2 also includes the experimental data obtained in NINA and NINA-2 (Bidoli et al., 2002) experiments.

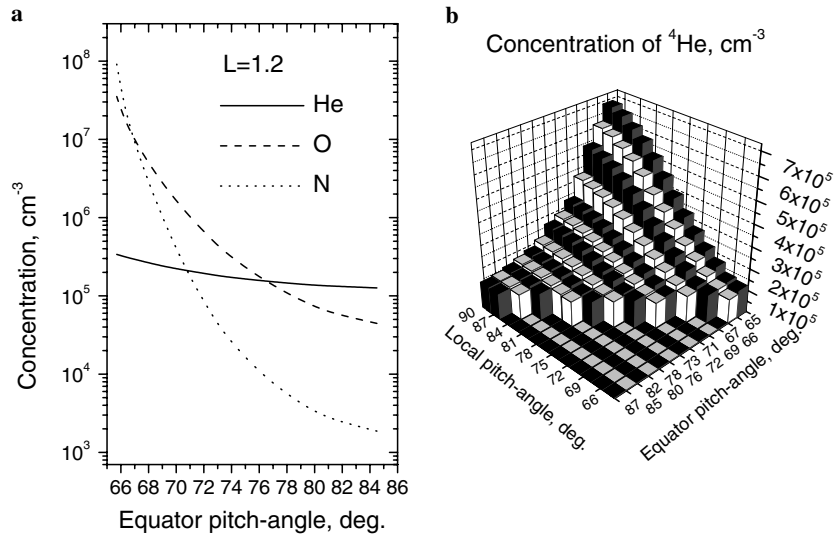


Fig. 1. Dependence of the drift-averaged concentrations of the main atmospheric constituents from an equator pitch-angle of trapped protons with energy 350 MeV (a). Dependence of the drift-averaged concentrations of atmospheric helium from the local and equator pitch-angle of trapped protons with energy 100 MeV (b) on L-shell 1.2.

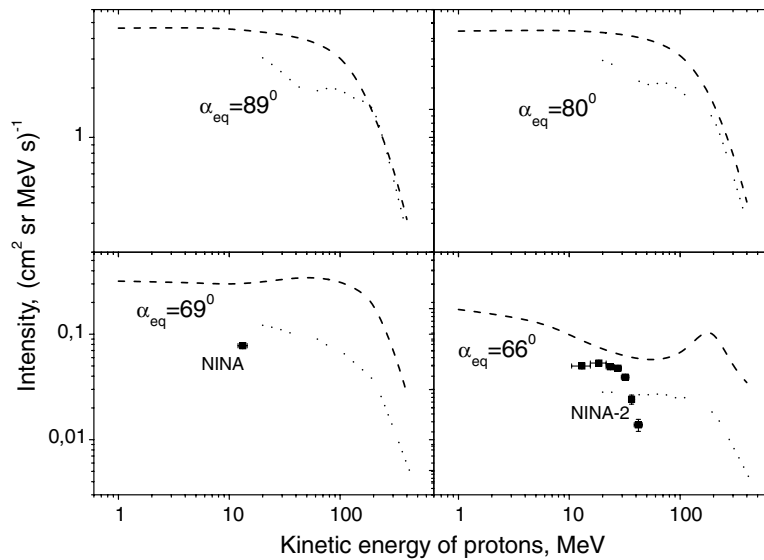


Fig. 2. Energetic directional spectrum of trapped protons for solar minimum at L-shell 1.2, defined from the AP-8 (dashed line) and SAMPEX/PET PSB97 (dotted line) models. Bottom figures also contain the experimental data obtained in RESURS-04/NINA and MITA/NINA-2 experiments.

3. Results

Described method was used to calculate the intensities of trapped high-energy ²H and ⁴He nuclei at L-shell < 1.3. To compare with experimental results the calculations were fulfilled for the values of equator pitch-angles, which covered by the measurements in NINA and NINA-2 experiments.

Fig. 3 represents data from RESURS-04/NINA experiment (Bakaldin et al., 2002) jointly with the intensity values of trapped ²H (a) and ⁴He (b) at L-shell 1.2 calculated using the AP-8 max proton fluxes (solid lines) and SAMPEX/PET PSB97 proton fluxes (dashed lines). Upper and lower curves correspond to equator pitch-angle 72°

and 66°, respectively. Equator pitch-angle distributions obtained in RESURS-04/NINA and MITA/NINA-2 experiments at L-shell 1.2 for trapped H (a) and He (b) are framing. More than 60% of events detected by NINA instrument have equator pitch-angles in the range from 66° to 72°, and the pitch-angles of more than 60% of events from NINA-2 experiment lie in the range from 64° to 70°.

Fig. 4 shows the contributions of the different atmospheric components (He, N and O) in the generation of high-energy trapped deuterium from SAMPEX/PET PSB97 proton fluxes for different equator pitch-angle values (a), (b) and (c) at L-shell 1.2. Total calculated deuterium intensities and data from RESURS-04/NINA (Bakaldin et al., 2002), MITA/NINA-2 and SAMPEX/

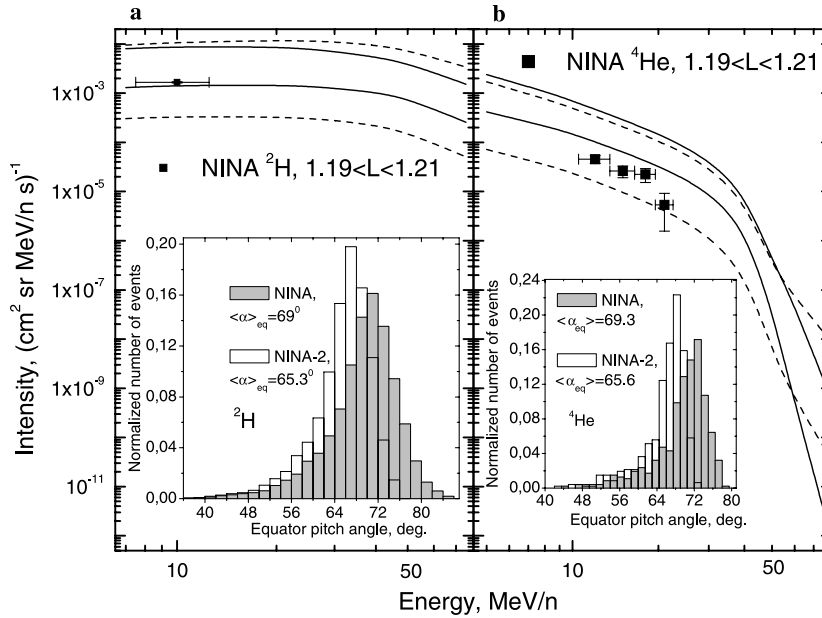


Fig. 3. The values of the intensity of trapped ^2H (a) and ^4He (b) at L-shell 1.2 calculated using the AP-8 max proton fluxes (solid lines) and SAMPEX/PET PSB97 proton fluxes (dashed lines). Upper and lower curves correspond to the equator pitch-angle 72° and 66° accordingly. Data from RESURS-04/NINA experiment are also shown. The distributions of equator pitch-angles obtained in RESURS-04/NINA and MITA/NINA-2 experiments at L-shell 1.2 for trapped H (a) and He (b) are framing. More than 60% of events detected by NINA instrument have equator pitch-angles in the range from 66° to 72° .

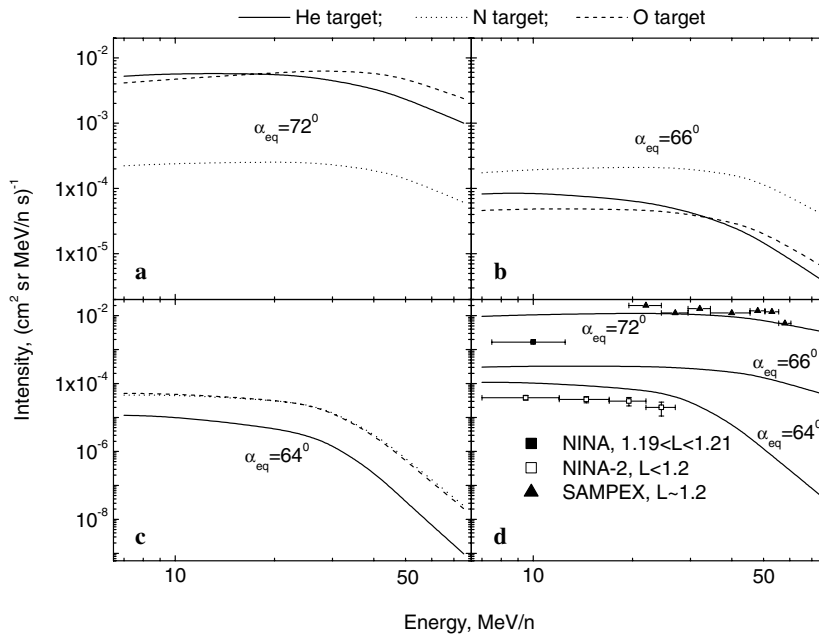


Fig. 4. The contributions of different atmospheric components (He, N and O) in the generation of high-energy trapped deuterium from SAMPEX/PET PSB97 proton fluxes for different equator pitch-angle values (a), (b), and (c) at L-shell 1.2. Total calculated deuterium intensities and data from the RESURS-04/NINA, MITA/NINA-2 and SAMPEX/PET experiments are also displayed (d).

PET (Selesnick and Mewaldt, 1996) experiments are also displayed (d).

The same results are shown in the Fig. 5 but for high-energy helium (^4He). Total calculated helium intensities and data from the RESURS-04/NINA (Bakaldin et al., 2002), MITA/NINA-2, SAMPEX/MAST (Selesnick and

Mewaldt, 1996) and CRRES/ONR-604 (Chen et al., 1996) experiments are presented in Fig. 5(d). The difference of the experimental values for CRRES/ONR-604 and analytical curves could be due to the influence of radial diffusion near $L \sim 1.3$ which has to be taken into account in the calculations (Pugacheva et al., 1998). Besides, the

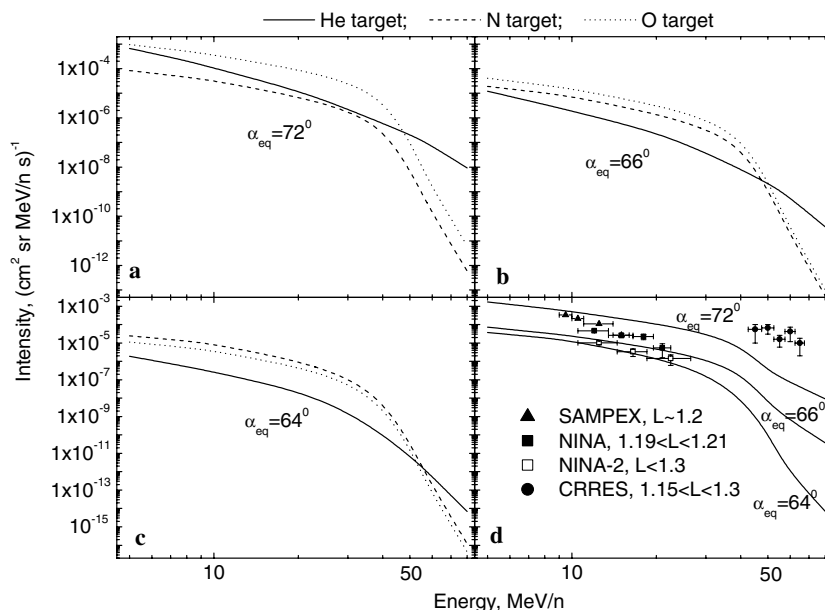


Fig. 5. The contributions of different atmospheric components (He, N, O) in the generation of high-energy trapped helium (^4He) from SAMPEX/PET PSB97 proton fluxes for different equator pitch-angle values (a), (b), (c) at L-shell 1.2. Total calculated helium intensities and data from RESURS-04/NINA, MITA/NINA-2, SAMPEX/MAST and CRRES/ONR-604 experiments are also displayed (d).

average value of the equator pitch-angle of trapped particles registered in CRRES experiment is higher $\sim 90^\circ$ than one used in the presented calculations.

The uncertainty involved in the calculations of production rate of secondary nuclei from Eq. (3) depends on uncertainties of the cross-sections ($\sim 10\%$), of the trapped proton fluxes model ($\sim 50\%$), of the averaged density of MSIS-90 model atmosphere ($\sim 15\%$) and of the numerical error of integration along the proton trajectory in Eq. (3) ($\sim 20\%$). Thus, a general uncertainty of source flux is $\sim 60\%$.

In the original work Selesnick and Mewaldt, 1996 the forward production of secondaries on the oxygen target was assumed. As a result, the difference with the calculations, reported above, becomes more than 100% at L-shell ~ 1.2 . Furthermore, they did not present the calculations of oxygen nuclear reactions for pitch-angles less than 80° at L-shell ~ 1.2 .

The comparison of calculated and experimental data taken during different solar activity phases reveals acceptable agreement and shows that the upper atmosphere is a sufficient source for the inner zone helium and heavy hydrogen isotopes. The best agreement between the calculations and experimental data comes if the SAMPEX/PET PSB97 model is used to evaluate the flux of trapped protons. However the worst case is the comparison of the $\text{He}4$ flux at high energy with the CRRES data. One possible explanation could be concerning with the fact, that for higher L-shells the radial diffusion becomes the significant source of trapped particles in this energy range and has to be taken into account. The calculation results are energy spectra and angular distributions of light nuclear isotopes in the inner radiation belt that may be used to develop

helium inner radiation belt model and to evaluate their contribution to SEU rates. To calculate the fluxes at higher L-shell the additional study of diffusion processes is needed (Pugacheva et al., 1998). Although AP-8 and SAMPEX/PSB97 may be publicly accessed through the SPENVIS, they exhibit an order of magnitude difference in low altitude proton fluxes (Heynderickx et al., 1999). So, to improve the accuracy of the calculations the more precise proton model is also claimed.

Acknowledgements

We thank M. Cyamukungu and S. Benck (Universite Catholique de Louvain, Center for Space Radiation, Belgium) for the help with cross-section data. This work was partially supported by INTAS Grant 1 03-55-1126 and by personal Grant of Russian president 1 MK-3796.2005.2.

References

- Bakaldin, A., Galper, A., Koldashov, S., et al. Geomagnetically trapped light isotopes observed with the detector NINA. *J. Geophys. Res.* 107 (A8), 1–8, 2002.
- Barton, C.E. Revision of international geomagnetic reference field released. *EOS Trans.* 77, 16, 1996.
- Bidoli, V., Casolino, M., De Pascale, M., et al. Energy spectrum of secondary protons above the atmosphere measured by the instruments NINA and NINA-2. *Ann. Geophysicae* 20, 1693–1697, 2002.
- Chen, J., Guzik, T.G., Wefel, J.P., et al. Energetic helium isotopes trapped in the magnetosphere. *J. Geophys. Res.* 101 (A11), 24787–24799, 1996.
- Dodd, P.E., Massengill, L.W. Basic mechanisms and modeling of Single-Event Upset in digital microelectronics. *IEEE Trans. Nucl. Sci.* 50 (3), 583–602, 2003.

- Gaffey, J., Bilitza, D. NASA/National Space Science Data Center trapped radiation models. *J. Spacecraft Rockets* 31 (2), 172, 1994.
- Galper, A.M., Kodashov, S.V., Leonov, A.A., et al. Light isotopes generation in the earth radiation belt. *Izvestiy RAN. Ser. Phys.* 67 (4), 525-529 (in Russian), 2003.
- Hedin, A.E. Extension of the MSIS thermospheric model into the middle and lower atmosphere. *J. Geophys. Res.* 96, 1159, 1991.
- Heynderickx, D., Kruglanski, M., Pierrard, V., Lemaire, J., Looper, M.D., Blake, J.B. A low altitude trapped proton model for solar minimum conditions based on SAMPEX/PET data. *IEEE Trans. Nucl. Sci.* 46, 1475, 1999.
- Jentsch, V., Wibberenz, G. An analytic study of the energy and pitch angle distribution of inner-zone protons. *J. Geophys. Res.* 85, 1-8, 1980.
- Pugacheva, G.I., Spjeldvik, W.N., Gusev, A.A., et al. Hydrogen and helium isotope inner radiation belts in the earth's magnetosphere. *Ann. Geophysicae* 16, 931-939, 1998.
- Selesnick, R.S., Mewaldt, R.A. Atmospheric production of radiation belt light isotopes. *J. Geophys. Res.* 101 (9), 19745-19757, 1996.
- Young, P.G., Arthur, E.D., Chadwick M.B., *Comprehensive Nuclear Model Calculations: Introduction to the Theory and Use of the GNASH Code*, LA-12343-MS, July 1992.